Desalination and Water Treatment
www.deswater.com

doi: 10.5004/dwt.2022.28928

274 (2022) 230–238
October

Adsorption of phosphate by Cu-loaded polyethylenimine modified wheat straw

Liuyan Han, Xu Liu*, Peifeng Yang, Runping Han*

College of Chemistry, Green Catalysis Center, Zhengzhou University, No 100 of Ke Xue Road, Zhengzhou 450001, China, emails: lxcod@zzu.edu.cn (X. Liu), rphan67@zzu.edu.cn (R. Han), hly1942404893@163.com (L. Han), 326105497@qq.com (P. Yang)

Received 13 April 2022; Accepted 22 September 2022

ABSTRACT

Excessive phosphate can cause eutrophication of water bodies and disturb the balance of water organisms while the exhausted adsorbent can be further utilized to bind adsorbate for second adsorption. In this study, wheat straw (WS) was modified by grafting polyethylenimine (PEI) and PEI-WS was obtained, then Cu^{2+}-loaded PEI-WS was used as adsorbent to bind phosphate (PO_4^{3-}) from solution in batch mode and fixed-bed column mode (as secondary adsorption). PEI is successfully modified onto surface of WS through elemental analysis. The results of batch experiments showed that the adsorption capacity of Cu-PEI-WS for toward PO_4^{3-} was 15.7 $mg \cdot g^{-1}$ (according to P) from experiments at 293 K. Adsorption isotherms were better fitted by Langmuir model and Temkin model while kinetic process was better fitted by Elovich model. The adsorption process was an exothermic spontaneous process. In column adsorption experiments, the effects of flow rate, column height and initial concentration of PO_4^{3-} on break-through curves were investigated and Thomas model was suitable to fit results of column adsorption. Secondary adsorption of spent adsorbents is one way of reuse about some material and plays an important role in environmental protection.

Keywords: Cu-PEI modified wheat straw; Adsorption; Phosphate

1. Introduction

Clean water is essential for life [1]. However, with the rapid economic development, smelting, electrolysis, electroplating, dye and other industries need to discharge a large amount of industrial wastewater every year [2–5]. If industrial wastewater is discharged into the environment without treatment, it will cause serious harm to the ecological environment, that's why more and more people are paying attention to wastewater treatment [6–8].

phosphate is a very important material in many industries [9]. Its widespread use in industry inevitably generates large amounts of phosphate-containing waste [10], which disturbs the biological balance in water, causes eutrophication of water bodies, and pollutes the environment [11,12]. The commonly used wastewater treatment methods are biological [12], oxidation [13,14], flocculation sedimentation [15] and adsorption method etc. In recent years, the main methods of phosphorus removal have been chemical and biological. Chemical phosphorus removal means that chemical reagents such as Fe^{3+} and Al^{3+} are added to the wastewater to produce phosphate precipitation by chemical reaction with phosphorus. Although the chemical precipitation method is highly efficient in removing phosphorus, it can cause re-pollution of the water body, and the treatment cost is high. The biological method uses functional microorganisms or algae to adsorb phosphorus. The disadvantage of the biological method of phosphorus removal is the high requirements for wastewater treatment technology and operating conditions, and the different water quality in various regions, which makes the implementation of this method difficult [16]. Adsorption is widely used for the removal of contaminants due to its simplicity and stability [3,4]. Baccar et al. [17] studied the activated carbon prepared by oxidation of

* Corresponding authors.

activated olive branches with potassium permanganate to improve its adsorption of metal ions. In the study, Cu^{2+} was used as the adsorbent, and by comparing before and after modification, it was found that the unit adsorption capacity of activated carbon increased from 12.0 to 35.3 $mg·g^{-1}$, which was a threefold increase. Sych et al. [18] prepared activated carbon by activating corn cob with phosphoric acid, so that the prepared activated carbon had phosphoric acid groups and a large number of carboxylic acid groups, ester groups and phenol groups on the surface, as well as a high specific surface area of 2,081 $m^2·g^{-1}$. The prepared modified adsorbent showed good removal of both copper ions and methylene blue.

Agricultural by-products such as cellulose and lignin are low-cost and abundant, and have a porous structure and large specific surface area [19], so they can be used as adsorbents. Wheat straw (WS) is rich in cellulose and lignin. However, the adsorption performance of natural wheat straw is poor. In order to improve the adsorption efficiency, straw modification has become critical. Mehdinejadiani et al. [20] made the attempt to chemically modify wheat straw with 3-chloropropyl to remove nitrate from water. The results showed that 85% nitrate removal was achieved when the solution pH = 7, the initial nitrate concentration was 20 $mg·L^{-1}$, and the MWS dosage was 2 $g·L^{-1}$.

Polyethylenimine (PEI) can be modified for the removal of pollutants from wastewater due to its high cationic and adsorptive properties and its ability to chelate with heavy metal ions, etc. [21]. PEI is a polymeric amine with good water solubility, so the modification needs to be combined with a cross-linking agent or through a grafting reaction to immobilize PEI on the surface of the adsorbent to avoid its loss. Sajab et al. [22] studied the modification of oil palm fruit shells with glutaraldehyde cross-linked PEI to obtain a cationic modifier to remove the anionic dye phenol red from water. The results showed that its maximum unit adsorption capacity was 108.7 $mg·g^{-1}$ at 293 K. Mao et al. [23] investigated the optimal modification conditions for PEI modification of glutamate fermentation waste biomass and performed adsorption studies using activated red as the adsorbent, and the results showed that the best adsorption effect was obtained by adding 4.29 g of PEI and 0.15 mL of glutaraldehyde to 10 g of biomass. The adsorption performance after modification was increased by 4.52 times without modification.

In our previous study, PEI modified WS was obtained by grafting epichlorohydrin (ECH) in NaOH solution without organic solvents, which is suitable to bind copper ion from solution [24]. In this study, the spent PEI-WS or Cu^{2+} loaded PEI-WS was used to bind phosphate as second adsorption from solution. Batch and dynamic adsorption studies were carried out, and the experimental data were fitted using adsorption models.

2. Materials and methods

2.1. Materials and reagents

Wheat straw (WS) was obtained from local countryside and WS (40–60 mesh was selected after pretreatment. Reagents: polyethylenimine (PEI), ethanol (C_2H_6O), epichlorohydrin (ECH), NaCl, Na_2SO_4, HCl, NaOH, KH_2PO_4, $CuSO_4·5H_2O$. The test reagents were all analytically pure, and the water used in the experiment was distilled water.

2.2. Preparation of Cu-PEI-WS

PEI-WS was prepared according to our previous study [24]. Fig. 1 shows the process of preparation. According to the adsorption results of PEI-WS on Cu^{2+}, the initial concentration of Cu^{2+} was selected to be 50 $mg·L^{-1}$, the solid–liquid ratio of adsorption was 0.8 $g·L^{-1}$. The reaction was carried out in a constant temperature oscillator for 3 h to allow PEI-WS to fully absorb Cu^{2+}. After filtration, the un-adsorbed copper ions on the surface were washed off with distilled water and dried. Cu-PEI-WS was prepared for secondary adsorption test toward phosphate. Adsorption quantity toward Cu^{2+} is 36.7 $mg·g^{-1}$ (PEI-WS). Cu-PEI-WS as adsorbent for secondary adsorption of PO_4^{3-} was carried out under various conditions [24].

2.3. Adsorption of phosphate by Cu-PEI-WS

2.3.1. Batch adsorption

A certain concentration of Cu-PEI-WS solution was taken into a small 50 mL conical flask and 10 mL of PO_4^{3-} solution of the desired concentration was added. The effects of temperature, concentration and time on the adsorption at 293, 303 and 313 K as well as the effects of pH and salinity on the adsorption of PO_4^{3-} were investigated. The changes of PO_4^{3-} solution concentration before and after adsorption were measured using molybdenum antimony spectrophotometric methods (at 700 nm) to calculate the unit adsorption amount.

The unit adsorption capacity q ($mg·g^{-1}$) and removal efficiency p (%) can be calculated by Eqs. (1) and (2). The adsorption experiments are carried out in triplicate and average results are recorded with errors less than 5%.

$$q = \frac{V\left(C_0 - C\right)}{m} \tag{1}$$

$$p = \frac{C_0 - C}{C_0} \times 100\% \tag{2}$$

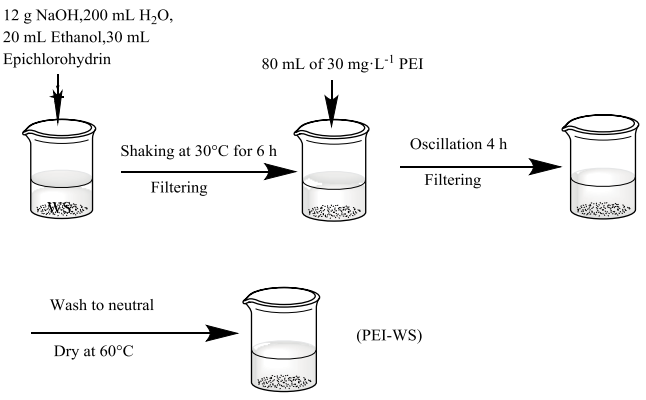

Fig. 1. Preparation process of PEI-WS.

where C_0 (mg·L^{-1}) and C are the concentration of PO_4^{3-} before and after adsorption, m is the mass (g) of adsorbent (Cu-PEI-WS).

2.3.2. Column adsorption

The dynamic adsorption experiments of Cu-PEI-WS on PO_4^{3-} were investigated according to the dynamic adsorption process of Cu^{2+} on PEI-WS [24]. A certain amount of Cu-PEI-WS was taken as the stationary phase in the adsorption column. A constant concentration of PO_4^{3-} solution was pumped into the column by a mobile pump, and the effluent was picked up at different times and its concentration was measured. The experimental conditions were as follows: (1) The initial concentration of PO_4^{3-} was 30 mg·L^{-1}, the flow rate was 6.8 mL·min^{-1}, and the column heights were set at 2.8, 5.2 and 7.0 cm to investigate the effect of column height on the adsorption results; (2) The flow rate was controlled to 6.8 mL·min^{-1}, the column height was 5.2 cm, and the initial concentrations of 15, 30 and 45 mg·L^{-1} of PO_4^{3-} solution were prepared to investigate the effect of initial concentration on the adsorption results; (3) The initial concentration of PO_4^{3-} was 30 mg·L^{-1}, the column height was 5.2 cm, and the flow rates were 8.5, 6.8 and 4.2 mL·min^{-1} to discuss the effect of flow rate on the dynamic adsorption of PO_4^{3-}. The dynamic penetration adsorption curves were plotted against t using C_t/C_0 (C_t and C_0 are the concentrations of PO_4^{3-} in the influent and effluent water) [25].

The value of the total mass of pollutants adsorbed, q_{total} (mg), can be estimated from the area beneath the breakthrough curve and the adsorption capacity, q_0 (mg·g^{-1}) is estimated using Eqs. (3) and (4), respectively.

$$q_{total} = \frac{v}{1{,}000}\int_{t=0}^{t=t_{total}} \left(C_0 - C_t\right)dt \tag{3}$$

$$q_0 = \frac{q_{total}}{x} \tag{4}$$

where C_0 is the concentration of phosphate in influent (mg·L^{-1}), x is the weight of dry adsorbent in the column (g), v is the flowing rate (mL·min^{-1}), t_{total} is the total flowing time (min), C_t is the concentration of adsorbate at a specified time.

3. Result and discussion

Elemental analysis showed that there were 3.20% N of PEI-WS and 0.12 N of WS. The isoelectric point of WS was 7.39 and the isoelectric point of PEI-WS was 8.38. Combining the results of FTIR [24], PEI is successfully modified onto surface of WS.

3.1. Batch adsorption

3.1.1. Effect of adsorbent dosage on secondary adsorption of PO_4^{3-}

In order to ensure the utilization of adsorbent, the effect of adsorbent dosage on the secondary adsorption of PO_4^{3-} was investigated using Cu-PEI-WS as adsorbent. It can be seen that when the adsorbent dosage gradually increased, the removal rate of PO_4^{3-} also gradually increased, while the unit adsorption amount gradually decreased (Fig. 2). This was because at first the amount of adsorbent added increased the more active sites that can adsorb PO_4^{3-}, and the removal rate increases; but as the amount of adsorbent increases, because the amount of PO_4^{3-} in the solution was certain, the active sites of each adsorbent cannot be completely combined, so the unit adsorption amount gradually decreased. The concentration of adsorbent was chosen to be 0.8 g·L^{-1} in order to achieve a high removal rate and a large unit adsorption capacity.

3.1.2. Effect of solution pH on secondary adsorption of phosphate

The effect of pH on the adsorption process was studied by adjusting the pH of the solution to 2–12 with certain concentrations of HCl and NaOH. It can be seen from the graph that the unit adsorption amount increased rapidly with the increase of pH under acidic conditions; the unit adsorption amount reached the maximum at pH = 6, and the unit adsorption amount remained basically unchanged at pH 6–8; the unit adsorption amount decreases gradually with the increase of pH under alkaline conditions, and remained basically unchanged after pH = 10 (Fig. 3). After consulting the ionization constant of phosphoric acid, it was known that at pH < 2, the main form of phosphate was H_3PO_4; between pH 2–4.5, the main form of $H_2PO_4^-$, H_3PO_4; between pH 5–9, the main form of $H_2PO_4^-$, HPO_4^{2-}; at pH > 10, the main form of HPO_4^{2-} and PO_4^{3-}. From the presence of phosphate forms, it can be assumed that the adsorption of Cu-PEI-WS toward PO_4^{3-} should be based on electrostatic attraction. When the pH was about 2, the unit adsorption amount was small, and it could be judged that the phosphate existed mainly in the form of molecules, and as the pH increased, $H_2PO_4^-$ ions appeared in the solution, and $H_2PO_4^-$ could be adsorbed on the surface of the adsorbent by electrostatic gravity, so the unit adsorption amount of PO_4^{3-} increased; after the pH was greater than 4.5, the phosphate in the solution existed in the form of negative charges The unit adsorption amount of

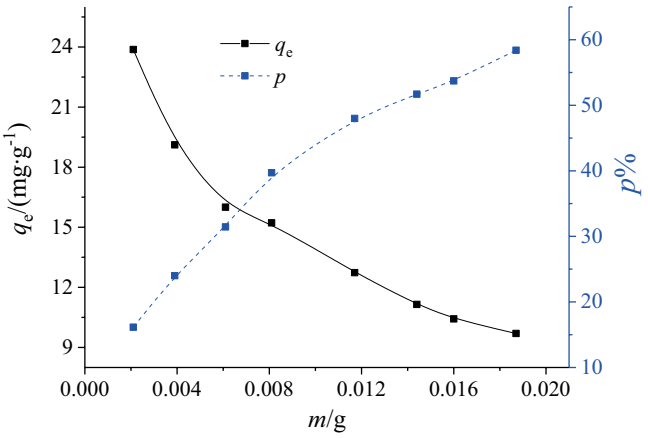

Fig. 2. Effect of adsorbent dosage on secondary adsorption of PO_4^{3-} (t = 480 min, C_0 = 30 mg·L^{-1}).

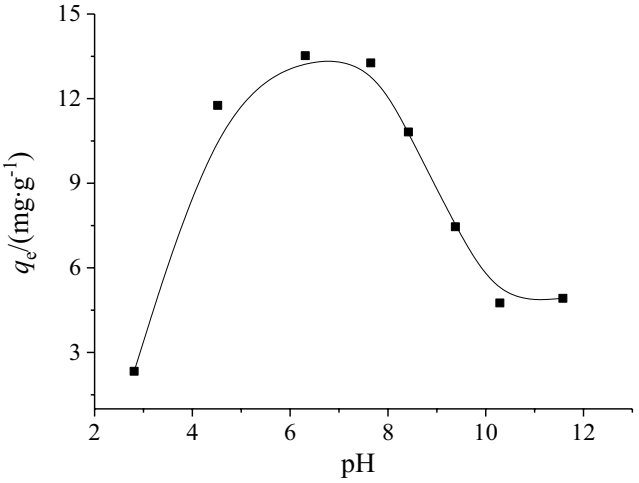

Fig. 3. Effect of solution pH on secondary adsorption of PO_4^{3-} (adsorbent dose = 0.8 g·L^{-1}, C_0 = 30 mg·L^{-1}, t = 180 min).

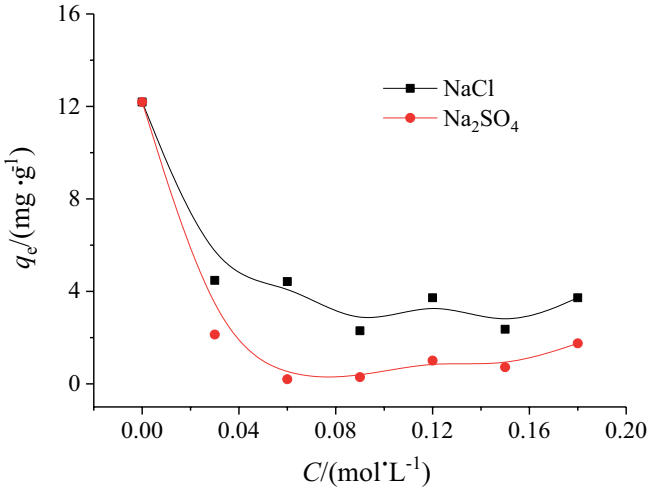

Fig. 4. Effect of co-existing ions on secondary adsorption of PO_4^{3-} (C_0 = 30 mg·L^{-1}, t = 180 min).

PO_4^{3-} increased; after the pH was greater than 4.5, the phosphate in solution was in the form of negative charge, so the unit adsorption amount reached the maximum; under the conditions of alkaline pH, OH^- competed with the negative ions containing phosphorus, so the unit adsorption amount gradually decreased. Finally, the adsorption test was carried out under neutral conditions. The practical application can be applied to wastewater with pH range of 5–8.

At low and high pH values, adsorption was not favored. Similar results have been observed in other studies, such as Congo red adsorption of on Al^{3+} and iminodiacetic acid modified magnetic peanut husk [25], fluoride adsorption on zirconium–carbon hybrid sorbent [26], p-nitrophenol adsorption on silver(I) triazole MOF [27].

3.1.3. Effect of co-existing ions on secondary adsorption of PO_4^{3-}

The effect of co-existing ions during the adsorption process should not be neglected. The effect of co-existing ions on secondary adsorption of PO_4^{3-} was investigated by adjusting the salt concentration with different masses of NaCl and Na_2SO_4. It can be seen from Fig. 4 that when the solution contains 0.03 mol·L^{-1} of inorganic salt ions, its unit adsorption amount decreases rapidly, and the effect of Na_2SO_4 is greater than that of NaCl.

From the results of the effect of salinity, if salinity has a large effect on adsorption, the adsorption mechanism is generally an electrostatic gravitational force between the adsorbent and the adsorbent mass. Zhang et al. studied the adsorption of phosphate from aqueous solutions by lanthanide-modified macroporous chelating resin. By studying the adverse effect of NaCl and Na_2SO_4 on adsorption, it was shown that the adsorbent and adsorbent masses interacted by electrostatic gravitational force [28]. In this experiment, the ionic strength has a negative effect because the increase in ionic concentration increases the ionic strength of the system and the ionic activity decreases, so it was not favorable for its adsorption, proving that the mechanism of adsorption in this reaction was electrostatic force between copper ions and phosphate on the surface of the adsorbent.

3.1.4. Adsorption isotherms for secondary adsorption of phosphate

The adsorption equilibrium of phosphate on q_e values was carried out at 293, 303 and 313 K, respectively. Then Plot the unit adsorption volume against the concentration in solution at equilibrium. From the results, it can be seen that the greater the concentration of adsorbate in solution at equilibrium, the greater its unit adsorption capacity. This phenomenon may be due to the increase in PO_4^{3-} concentration resulting in increased mass transfer of PO_4^{3-} to the adsorbent surface. The effect of temperature on adsorption was not significant. It is favorable to the adsorption at higher temperature and this adsorption reaction was exothermic. The adsorption capacity from experiments was to 15.7, 15.2, and 14.8 mg·g^{-1} at 293, 303, and 313 K, respectively.

The common adsorption isotherm models Langmuir, Freundlich, and Temkin were used to describe the adsorption behavior. The results of the fit are shown in Fig. 5.

Langmuir model is expressed as following equation [29]:

$$q_e = \frac{q_m K_L C_e}{1 + K_L C_e} \tag{3}$$

Freundlich model is presented as following equation [30]:

$$q_e = K_F C_e^{1/n} \tag{4}$$

Temkin model is expressed as following equation [31]:

$$q_e = A + B \ln C_e \tag{5}$$

where C_e is the PO_4^{3-} concentration at equilibrium (mg·L^{-1}), q_m (mg·g^{-1}) is the maximum adsorption amount; K_L (L·mg^{-1}) and a constant related to the adsorption energy; K_F and $1/n$

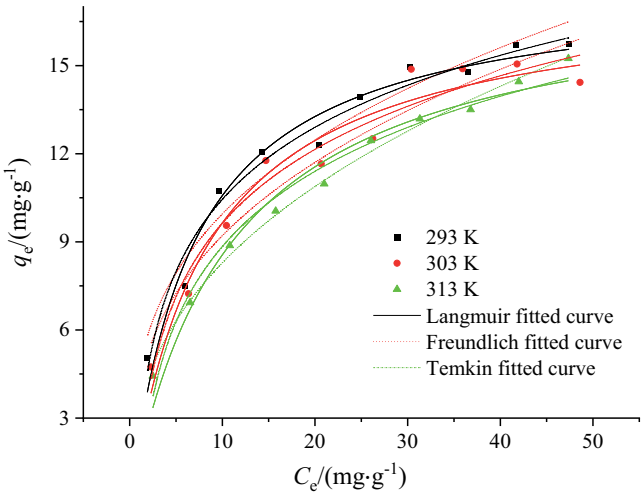

Fig. 5. Fitting curves of different isotherm models for Cu-PEI-WS adsorption of PO_4^{3-} (t = 180 min).

are Freundlich parameters related to the adsorption capacity of the adsorbent and the adsorption strength A and B are constants of mode.

Nonlinear regression analysis was used to obtain the parameters and decidable coefficients R^2 and differential sum SAE of the corresponding models with the least differential sum, and the results are listed in Table 1.

The results showed that the Langmuir model and Temkin model were better fitted, with R^2 above 0.951. In this adsorption process, the Langmuir model fits better, indicating that monomolecular layer adsorption accounts for the major part of this adsorption process. The R^2 of the Freundlich model fit was also higher, which proved that there is also multilayer adsorption in this adsorption process. The Temkin model was used to describe the adsorption on inhomogeneous surfaces, which can be presumed to be inhomogeneous in the adsorption process. The maximum adsorption capacity from Langmuir model at 293, 303, and 313 K was 17.8, 16.6, and 15.8 mg·g^{-1}.

3.1.5. Kinetics study of secondary adsorption toward phosphate

The adsorption equilibrium of c (initial concentration of 30 mg·L^{-1}) on q_e value was carried out at different times and plotted as q_e vs. t. It can be seen that the higher the temperature is, the less favorable the adsorption of PO_4^{3-}, indicating that this adsorption reaction is exothermic.

The adsorption kinetics was studied to further analyze the adsorption mechanism. In this experiment, the pseudo-first-order kinetic model, Elovich kinetic model, and double constant kinetic model were used for nonlinear fitting. The fitted curves are shown in Fig. 6, and the fitted parameters of each model are shown in Table 2.

The expression of pseudo-first-order kinetic model is as follows [32]:

$$q_t = q_e\left(1 - e^{-k_1 t}\right) \tag{6}$$

where k_1 is the rate constant (min^{-1}).

The expression of Elovich equation is as follows [33]:

$$q_t = \frac{\ln(\alpha\beta)}{\beta} + \frac{\ln t}{\beta} \tag{7}$$

where α is the initial adsorption rate constant (mg·g^{-1}·min^{-1}) while β is related to the extent of surface coverage and activation energy for chemisorption (g·mg^{-1}).

By comparing the fitted curves of each model and the R^2 and error analysis results of each model, it was found

Table 1
Fitting parameters for each isotherm model of Cu-PEI-WS^{2+} adsorption PO_4^{3-}

Langmuir						
T (K)	$q_{e(\exp)}$ (mg·g^{-1})	K_L (L·mg^{-1})	$q_{m(\text{theo})}$ (mg·g^{-1})	R^2	SAE	ARS × 10^{-3}
313	14.8	0.0927 ± 0.013	15.8 ± 0.8	0.970	4.11	4.49
303	15.2	0.122 ± 0.021	16.6 ± 0.8	0.951	6.49	3.85
293	15.7	0.146 ± 0.021	17.8 ± 0.6	0.966	4.59	4.65
Freundlich						
T (K)	$q_{e(\exp)}$ (mg·g^{-1})	K_F	$1/n$	R^2	SAE	ARS × 10^{-3}
313	14.8	3.36 ± 0.14	0.393 ± 0.013	0.994	2.11	0.688
303	15.2	4.17 ± 0.54	0.345 ± 0.038	0.929	6.88	4.41
293	15.7	4.72 ± 0.44	0.324 ± 0.028	0.956	6.20	3.60
Temkin						
T (K)	$q_{e(\exp)}$ (mg·g^{-1})	A	B	R^2	SAE	ARS × 10^{-4}
313	14.8	0.371 ± 0.52	3.68 ± 0.17	0.981	8.11	13.6
303	15.2	1.33 ± 0.82	3.61 ± 0.27	0.951	1.99	1.28
293	15.7	2.33 ± 0.58	3.53 ± 0.19	0.974	4.15	6.86

that the R^2 of the Elovich model fitted at different temperatures and concentrations was above 0.827, which was a good fit. The R^2 fitted by the pseudo-first-order model was smaller at higher and lower concentrations, but the R^2 fitted by the pseudo-first-order model was larger at different temperatures at 30 mg·L^{-1}, which was in good agreement. The differences between the fitted q_e of the observed models and the experimental values were small, and the errors were within 4%, and the fitted results were almost error-free at 303 K and 30 mg·L^{-1}. When the pseudo-first-order kinetic model is fit, it indicates that the adsorption is controlled by external mass transfer [34].

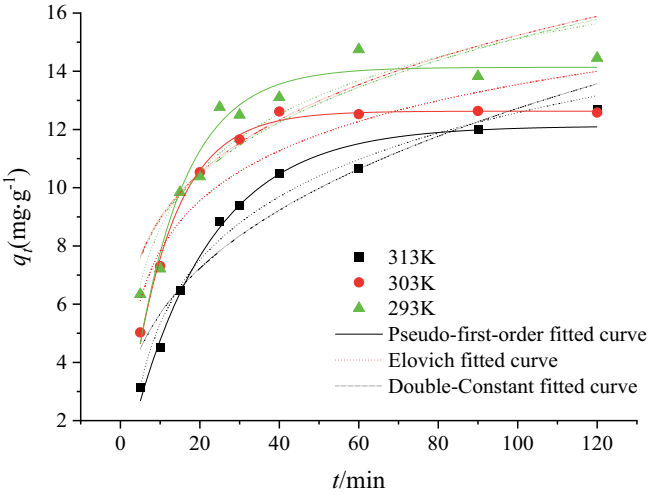

Fig. 6. Fitting curves of kinetic models for Cu-PEI-WS adsorption of PO_4^{3-} (m = 0.008 g, C_0 = 30 mg·L^{-1}, pH = 6).

3.1.6. Analysis of thermodynamic results

Through the study of some thermodynamic parameters, we can derive the possibility of the adsorption reaction occurring and the degree of occurrence have a more comprehensive understanding of the adsorption process, it is necessary to carry out some calculations of thermodynamic data, the parameters that often need to be calculated are $\Delta G°$, $\Delta H°$, $\Delta S°$, and their calculation formulae are as follows [35]:

$$\Delta G° = -RT\ln K_c \tag{8}$$

$$\Delta G° = \Delta H° - T\Delta S° \tag{9}$$

where K_c ($C_{ad,e}/C_e$) is the apparent adsorption equilibrium constant, where $C_{ad,e}$ is the concentration of adsorbate on the adsorbent when adsorption reaches equilibrium and C_e is the concentration of adsorbate in solution at equilibrium, using concentration instead of activity to find the adsorption equilibrium constant of the system. R is the gas constant (8.314 J·mol^{-1}·K^{-1}); T is the absolute temperature (K).

The activation energy represents the energy barrier that needs to be overcome for a chemical reaction to occur

Table 2
Kinetic fitting parameters of each model for Cu-PEI-WS^{2+} adsorption of PO_4^{3-}

Pseudo-first-order equation							
T (K)	C_0 (mg·L^{-1})	$q_{e(exp)}$ (mg·g^{-1})	k_1 (min^{-1})	q_e (mg·g^{-1})	R^2	SAE	ARS × 10^{-3}
303	45	15.0	0.168 ± 0.023	14.4 ± 0.4	0.765	6.47	2.56
303	30	12.6	0.0914 ± 0.037	12.6 ± 0.1	0.993	15.9	2.46
303	15	9.06	0.0685 ± 0.0140	9.02 ± 0.6	0.692	7.14	15.6
313	30	11.9	0.0498 ± 0.0360	12.1 ± 0.3	0.982	2.49	1.72
293	30	13.8	0.0798 ± 0.0085	14.1 ± 0.4	0.924	5.85	4.57
Elovich equation							
T (K)	C_0 (mg·L^{-1})	$q_{e(exp)}$ (mg·g^{-1})	α	β	R^2	SAE	ARS × 10^{-3}
303	45	15.0	139	0.577	0.828	20.1	7.16
303	30	12.6	5.83	0.403	0.843	7.34	4.80
303	15	9.06	3.70	0.569	0.878	5.76	1.29
313	30	11.9	1.71	0.318	0.968	4.00	2.58
293	30	13.8	5.94	0.353	0.871	8.16	3.92
Double constant equation							
T (K)	C_0 (mg·L^{-1})	$q_{e(exp)}$ (mg·g^{-1})	Ks	a	R^2	SAE	ARS × 10^{-3}
303	45	15.0	0.124 ± 0.022	8.78 ± 0.71	0.785	4.71	2.98
303	30	12.6	0.221 ± 0.053	4.87 ± 1.0	0.752	9.21	10.7
303	15	9.06	0.248 ± 0.031	3.05 ± 0.37	0.881	6.49	1.74
313	30	11.9	0.351 ± 0.046	2.53 ± 0.48	0.901	7.05	14.5
293	30	13.8	0.231 ± 0.040	5.23 ± 0.80	0.805	10.3	7.21

and represents the minimum amount of energy required for a chemical reaction to occur. The smaller the activation energy, the more likely the reaction will occur. It is calculated by the following formula.

$$\ln k = -\frac{E_a}{RT} + \ln A \tag{11}$$

where A is the temperature effect factor, K is the adsorption rate constant and E_a is the apparent activation energy of the reaction (kJ·mol^{-1}).

Thermodynamic data of secondary adsorption of phosphate were obtained by thermodynamic equations, and the results are shown in Table 3. From Table 3, it can be obtained that $\Delta G° < 0$, indicating that the adsorption was a spontaneous process. The absolute value of $\Delta G°$ becomes smaller as the temperature increases, indicating that the higher the temperature the less spontaneous it occurs, and increasing the temperature is not conducive to its adsorption. $\Delta H° < 0$, proving that the secondary adsorption of PO_4^{3-} was an exothermic reaction, and increasing the temperature was not conducive to adsorption, which was consistent with the conclusion obtained from the discussion of $\Delta G°$. $\Delta S° < 0$, proved that this adsorption process was a process of entropy reduction. E_a was 16.1 kJ·mol^{-1}, proving that the adsorption process occurring in this process was mainly physical adsorption.

3.2. Adsorption in column mode

3.2.1. Breakthrough curve of PO_4^{3-} on Cu-PEI-WS

Secondary adsorption of PO_4^{3-} by Cu-PEI-WS can be further demonstrated by column adsorption.

From Fig. 7a it can be seen that as the column height increased from 2.8 to 7.0 cm, the breakthrough time increased from 5 to 30 min, and the time to reach adsorption saturation also increased sequentially from 60 to 140 min. This was because when the column height increased, the adsorbed mass in the column increased, thus the adsorption active site increased and the residence time of the adsorbed mass increased, which slowed down the breakthrough of the adsorption column and facilitated increase the recovery of PO_4^{3-}. From Fig. 7b it can be seen that the greater the concentration, the shorter the breakthrough time. The breakthrough time was 15 min at the initial concentration of 45 mg·L^{-1}, while the breakthrough time was 30 min at the initial concentration of 15 mg·L^{-1}. The breakthrough time decreased with the increase of concentration. When the adsorbent content in the solution increased, the concentration driving force increased, the mass transfer rate increased, and then the slope of the breakthrough curve becomes larger and the breakthrough time is shortened [36]. As can be seen from Fig. 7c, the higher the flow rate, the shorter the breakthrough time and the shorter the time to reach adsorption saturation. The higher the flow rate was, the less favorable it was for adsorption. This was because the higher the flow rate, the shorter the residence time of the adsorbent in the column and the shorter the contact

Table 3
Thermodynamic parameters of PO_4^{3-} adsorption

E_a (kJ·mol^{-1})	ΔH (kJ·mol^{-1})	ΔS (J·mol^{-1}·K^{-1})	ΔG (kJ·mol^{-1})		
			303 K	313 K	323 K
16.1	–12.9	–40.9	–0.877	–0.492	–0.0597

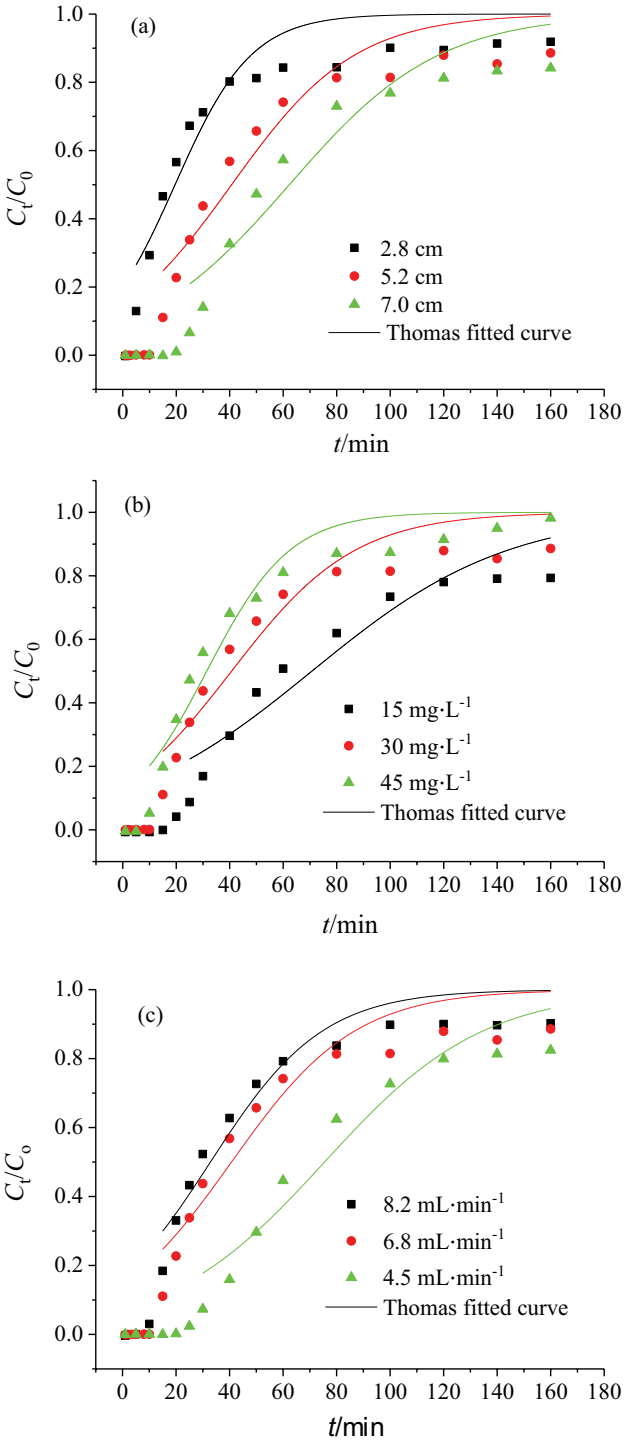

Fig. 7. Experimental results of column adsorption and fitting curves of Thomas model.

Table 4
Fitted results of Thomas model

Z (cm)	v (mL·min^{-1})	C_0 (mg·L^{-1})	k_{Th} (mL·mg^{-1}·min^{-1})	$q_{0(cal)}$ (mg·g^{-1})	q_0 (mg·g^{-1})	R^2	SAE	ARS × 10^{-2}
2.8	6.8	30	2.33 ± 0.47	13.3 ± 1.5	23.0	0.859	1.09	2.60
5.2	6.8	30	1.44 ± 0.27	15.8 ± 1.4	20.5	0.881	0.688	15.0
7.0	6.8	30	1.19 ± 0.24	15.8 ± 1.3	17.6	0.875	0.579	29.8
5.2	4.5	30	1.12 ± 0.18	36.7 ± 2.3	20.5	0.914	0.402	14.4
5.2	8.2	30	1.59 ± 0.26	7.92 ± 0.63	21.1	0.912	0.542	2.08
5.2	6.8	15	1.82 ± 0.30	13.8 ± 1.0	29.5	0.889	0.436	15.0
5.2	6.8	45	1.43 ± 0.24	18.3 ± 1.3	16.0	0.926	0.651	34.3

time with the adsorbent, and thus the shorter the breakthrough time. Under high flow rate conditions, the faster the adsorbate transport, the faster the adsorption rate and the easier it was to reach adsorption saturation [37].

3.2.2. Thomas model application

The kinetic results of the experiments were analyzed using Thomas model and Yan model for secondary adsorption PO_4^{3-} dynamic tests.

$$\frac{C_t}{C_0} = \frac{1}{1+\exp\left(\frac{k_{Th}q_0x}{v-k_{Th}C_0t}\right)} \tag{12}$$

where C_t and C_0 are the effluent and influent pollutants concentration (mg·L^{-1}), k_{Th} is the Thomas rate constant (mL·min^{-1}·mg^{-1}), q_0 is the maximum adsorption quantity (mg·g^{-1}), x is the weight of material (g), V_{eff} (vt) is the effluent volume (mL) and v is the flowing time (mL·min^{-1}).

The results of its nonlinear fitting are also shown in Fig. 7. The fitted parameters of the model are shown in Table 4.

The Thomas model fitted the breakthrough curve when the C_t/C_0 is greater than 0.05. Fig. 7 shows the breakthrough curve, and by fitting the model parameters in the plot and Table 4, it was shown that the Thomas model can describe the adsorption behavior better, and the fitted R^2 are above 0.859. The observed parameter k_{Th} decreases with increasing column height and increases with increasing flow rate. The experimentally obtained values of $q_{0(cal)}$ are some differences from the values of $q_{e(exp)}$ calculated by Eq. (4).

3.3. Potential application of spent adsorbent

Recovery of adsorbate from solution or reuse of spent adsorbent is important as this can make the adsorption process economical [38–41]. Quaternary ammonium modified sugarcane bagasse as anionic exchanger can adsorb phosphate from solution and the P-loaded adsorbent was further treated as a slow-release phosphate fertilizer in water or soil [42]. In this study, there are nutrient elements (N and P) and micronutrient element (Cu, essential element in biological body) about P-loaded Cu-PEI-WS. So maybe this spent material can be used as soil amendment. The application of this spent adsorbent can be performed in future study.

4. Conclusion

Cu-PEI-WS used as adsorbent for secondary adsorption of PO_4^{3-} was carried out under neutral pH conditions. The pH was not favorable for the adsorption under both over-acid and over-base conditions, and the presence of inorganic salt ions was not favorable for the adsorption. The secondary PO_4^{3-} adsorption process was exothermic and the increase in temperature was not favorable for the adsorption reaction. The Langmuir model was better to fit the equilibrium data and this indicated monomolecular layer adsorption for the major part of this adsorption process. The Elovich model was best to predict the kinetic process. Thomas model could describe the adsorption behavior of column mode. In summary, Cu-PEI-WS can be used as an adsorbent for secondary adsorption of phosphate.

Acknowledgements

This work was financially supported by the Henan province basis and advancing technology research project (142300410224).

References

[1] S. Ghosh, A. Malloum, C.A. Igwegbe, J.O. Ighalo, S. Ahmadi, M.H. Dehghani, A. Othmani, O. Gökkuş, N.M. Mubarak, New generation adsorbents for the removal of fluoride from water and wastewater: a review, J. Mol. Liq., 346 (2022) 118257, doi: 10.1016/j.molliq.2021.118257.
[2] A. Shafique, Removal of toxic pollutants from aqueous medium through adsorption: a review, Desal. Water Treat., 234 (2021) 38–57.
[3] F.M. Mpatani, A.A. Aryee, A.N. Kani, R.P. Han, Z.H. Li, E. Dovi, L.B. Qu, A review of treatment techniques applied for selective removal of emerging pollutant-trimethoprim from aqueous systems, J. Cleaner Prod., 308 (2021) 127359, doi: 10.1016/j.jclepro.2021.127359.
[4] A.A. Aryee, F.M. Mpatani, A.N. Kani, E. Dovi, R.P. Han, Z.H. Li, L.B. Qu, A review on functionalized adsorbents based on peanut husk for the sequestration of pollutants in wastewater: Modification methods and adsorption study, J. Cleaner Prod., 310 (2021) 127502, doi: 10.1016/j.jclepro.2021.127502.
[5] N.Y. Donkadokula, A.K. Kola, I. Naz, D. Saroj, A review on advanced physico-chemical and biological textile dye wastewater treatment techniques, Rev. Environ. Sci. Biotechnol., 19 (2020) 543–560.
[6] O. Lefebvre, R. Moletta, Treatment of organic pollution in industrial saline wastewater: a literature review, Water Res., 40 (2006) 3671–3682.
[7] A. Nasar, F. Mashkoor, Application of polyaniline-based adsorbents for dye removal from water and wastewater—a review, Environ. Sci. Pollut. Res., 26 (2019) 5333–5356.

[8] S. Li, Y. Chen, X. Pei, S. Zhang, X. Feng, J. Zhou, B. Wang, Water purification: adsorption over metal-organic frameworks, Chin. J. Chem., 34 (2016) 175–185.
[9] M. Schorr, B. Valdez, The phosphoric acid industry: equipment, materials, and corrosion, Corros. Rev., 34 (2016) 85–102.
[10] T.L. Eberhardt, S.H. Min, Biosorbents prepared from wood particles treated with anionic polymer and iron salt: effect of particle size on phosphate adsorption, Bioresour. Technol., 99 (2008) 626–630.
[11] T. Sheng, Z. Zhang, Y. Hu, Y. Tao, J. Zhang, Z. Shen, J. Feng, A. Zhang, Adsorption of phosphorus by using magnetic Mg–Al-, Zn–Al- and Mg–Fe-layered double hydroxides: comparison studies and adsorption mechanism, Environ. Sci. Pollut. Res., 26 (2019) 7102–7114.
[12] G. Chen, R. Bai, Y. Zhang, B. Zhao, Y. Xiao, Application of metagenomics to biological wastewater treatment, Sci. Total Environ., 807 (2022) 150737, doi: 10.1016/j.scitotenv.2021.150737.
[13] R.S. Lankone, K.E. Challis, Y. Bi, D. Hanigan, R.B. Reed, T. Zaikova, J.E. Hutchison, P. Westerhoff, J. Ranville, H. Fairbrother, L.M. Gilbertson, Methodology for quantifying engineered nanomaterial release from diverse product matrices under outdoor weathering conditions and implications for life cycle assessment, Environ. Sci.: Nano, 4 (2017) 1784–1797.
[14] Y.N. Shang, X. Xu, Q.Y. Yue, B.Y. Gao, Y.W. Li, Nitrogen-doped carbon nanotubes encapsulating Fe/Zn nanoparticles as a persulfate activator for sulfamethoxazole degradation: role of encapsulated bimetallic nanoparticles and nonradical reaction, Environ. Sci.: Nano, 7 (2020) 1444–1453.
[15] D.M. Formentini-Schmitt, M.R. Fagundes-Klen, M.T. Veit, S.M. Palácio, D.E.G. Trigueros, R. Bergamasco, G.A.P. Mateus, Potential of the *Moringa oleifera* saline extract for the treatment of dairy wastewater: application of the response surface methodology, Environ. Technol., 40 (2019) 2290–2299.
[16] B.L. Wu, J. Wan, Y.Y. Zhang, B.C. Pan, I.M.C. Lo, Selective phosphate removal from water and wastewater using sorption: process fundamentals and removal mechanisms, Environ. Sci. Technol., 54 (2020) 50–66.
[17] R. Baccar, J. Bouzid, M. Feki, A. Montiel, Preparation of activated carbon from Tunisian olive-waste cakes and its application for adsorption of heavy metal ions, J. Hazard. Mater., 162 (2009) 1522–1529.
[18] N.V. Sych, S.I. Trofymenko, O.I. Poddubnaya, M.M. Tsyba, V.I. Sapsay, D.O. Klymchuk, A.M. Puziy, Porous structure and surface chemistry of phosphoric acid activated carbon from corncob, Appl. Surf. Sci., 261 (2012) 75–82.
[19] Y. Cao, W. Xiao, G. Shen, G. Ji, Y. Zhang, C. Gao, L. Han, Carbonization and ball milling on the enhancement of Pb(II) adsorption by wheat straw: competitive effects of ion exchange and precipitation, Bioresour. Technol., 273 (2019) 70–76.
[20] B. Mehdinejadiani, S.M. Amininasab, L. Manhooei, Enhanced adsorption of nitrate from water by modified wheat straw: equilibrium, kinetic and thermodynamic studies, Water Sci. Technol., 79 (2019) 302–313.
[21] A.N. Kani, E. Dovi, F.M. Mpatani, A.A. Aryee, R.P. Han, Z.H. Li, L.B. Qu, A review of pollutant decontamination by polyethylenimine engineered agricultural waste materials, Environ. Chem. Lett., 20 (2022) 705–729.
[22] M.S. Sajab, C.H. Chia, S. Zakaria, P.S. Khiew, Cationic and anionic modifications of oil palm empty fruit bunch fibers for the removal of dyes from aqueous solutions, Bioresour. Technol., 128 (2013) 571–577.
[23] J. Mao, I.S. Kwak, M. Sathishkumar, K. Sneha, Y.-S. Yun, Preparation of PEI-coated bacterial biosorbent in water solution: optimization of manufacturing conditions using response surface methodology, Bioresour. Technol., 102 (2011) 1462–1467.
[24] J.J. Dong, Y.Y. Du, R.S. Duyu, Y. Shang, S.S. Zhang, R.P. Han, Adsorption of copper ion from solution by polyethylenimine modified wheat straw, Bioresour. Technol. Rep., 6 (2019) 96–102.
[25] A.A. Aryee, E. Dovi, R.P. Han, Z.H. Li, L.B. Qu, One novel composite based on functionalized magnetic peanut husk as adsorbent for efficient sequestration of phosphate and Congo red from solution: characterization, equilibrium, kinetic and mechanism studies, J. Colloid Interface Sci., 598 (2021) 69–82.
[26] L.H. Velazquez-Jimenez, R.H. Hurt, J. Matos, J.R. Rangel-Mendez, Zirconium–carbon hybrid sorbent for removal of fluoride from water: oxalic acid mediated Zr(IV) assembly and adsorption mechanism, Environ. Sci. Technol., 48 (2014) 1166–1174.
[27] H. Miao, S. Song, H. Chen, W. Zhang, R. Han, G. Yang, Adsorption study of p-nitrophenol on a silver(I) triazolate MOF, J. Porous Mater., 27 (2020) 1409–1417.
[28] X.T. Zhang, C.H. Ma, K. Wen, R.P. Han, Adsorption of phosphate from aqueous solution by lanthanum modified macroporous chelating resin, Korean J. Chem. Eng., 37 (2020) 766–775.
[29] I. Langmuir, The adsorption of gases on plane surfaces of glass, mica and platinum, J. Am. Chem. Soc., 40 (1918) 1361–1403.
[30] C. Na, Size-controlled capacity and isocapacity concentration in Freundlich adsorption, ACS Omega, 5 (2020) 13130–13135.
[31] C.J. Pursell, H. Hartshorn, T. Ward, B.D. Chandler, F. Boccuzzi, Application of the Temkin model to the adsorption of CO on gold, J. Phys. Chem., C, 115 (2011) 23880–23892.
[32] J. Lin, L. Wang, Comparison between linear and non-linear forms of pseudo-first-order and pseudo-second-order adsorption kinetic models for the removal of methylene blue by activated carbon, Front. Environ. Sci. Eng., 3 (2009) 320–324.
[33] F. Chen, C. Zhou, G. Li, F. Peng, Thermodynamics and kinetics of glyphosate adsorption on resin D301, Arabian J. Chem., 9 (2016) S1665–S1669.
[34] H. Wang, Y. Duan, Z. Ying, Y. Xue, Effects of SO_2 on Hg adsorption by activated carbon in O_2 /CO_2 conditions. Part 1: Experimental and kinetic study, Energy Fuels, 32 (2018) 10773–10778.
[35] W. Konicki, M. Aleksandrzak, D. Moszyński, E. Mijowska, Adsorption of anionic azo-dyes from aqueous solutions onto graphene oxide: equilibrium, kinetic and thermodynamic studies, J. Colloid Interface Sci., 496 (2017) 188–200.
[36] Z. Akzu, F. Gonen, Biosorption of phenol by immobilized activated sludge in a continuous packed bed: prediction of breakthrough curves, Process Biochem., 39 (2004) 599–613.
[37] J.L. Wang, X. Liu, M.M. Yang, H.Y. Han, S.S. Zhang, G.F. Ouyang, R.P. Han, Removal of tetracycline using modified wheat straw from solution in batch and column modes, J. Mol. Liq., 338 (2021) 116698, doi: 10.1016/j.molliq.2021.116698.
[38] G.J. Jiao, J.L. Ma,, Y.C. Li, D.N. Jin, Z. Ali, J.H. Zhou, R.C. Sun, Recent advances and challenges on removal and recycling of phosphate from wastewater using biomass-derived adsorbent, Chemosphere, 278 (2021) 130377, doi: 10.1016/j.chemosphere.2021.130377.
[39] T.J. Al-Musawi, N. Mengelizadeh, F. Ganji, C.Q. Wang, D. Balarak, Preparation of multi-walled carbon nanotubes coated with $CoFe_2O_4$ nanoparticles and their adsorption performance for Bisphenol A compound, Adv. Powder Technol., 33 (2022) 103438, doi: 10.1016/j.apt.2022.103438.
[40] A.A. Aryee, R.P. Han, A novel biocomposite based on peanut husk with antibacterial properties for the efficient sequestration of Trimethoprim in solution: batch and column adsorption studies, Colloids Surf., A, 635 (2022) 128051, doi: 10.1016/j.colsurfa.2021.128051.
[41] F.K. Mostafapour, M. Yilmaz, A.H. Mahvi, A. Younesi, F. Ganji, D. Balarak, Adsorptive removal of tetracycline from aqueous solution by surfactant-modified zeolite: equilibrium, kinetics and thermodynamics, Desal. Water Treat., 247 (2022) 216–228.
[42] Y.N. Shang, K.Y. Guo, P. Jiang, X. Xu, B.Y. Gao, Adsorption of phosphate by the cellulose-based biomaterial and its sustained release of laden phosphate in aqueous solution and soil, Int. J. Biol. Macromol., 109 (2018) 524–534.